optica

# Direct measurement of quantum efficiency of single-photon emitters in hexagonal boron nitride: supplemental material

NIKO NIKOLAY[1,2,*], NOAH MENDELSON[3], ERSAN ÖZELCI[1,2], BERND SONTHEIMER[1,2], FLORIAN BÖHM[1,2], GÜNTER KEWES[1,2], MILOS TOTH[3], IGOR AHARONOVICH[3,*], AND OLIVER BENSON[1,2]

[1]AG Nanooptik, Humboldt-Universität zu Berlin, Newtonstraße 15, D-12489 Berlin, Germany
[2]IRIS Adlershof, Humboldt-Universität zu Berlin, Zum Großen Windkanal 6, 12489 Berlin, Germany
[3]School of Mathematical and Physical Sciences, University of Technology Sydney, Ultimo, New South Wales 2007, Australia
[*]Corresponding authors: nikolay@physik.hu-berlin.de and Igor.Aharonovich@uts.edu.au

Published 20 August 2019

**This document provides supplementary information to "Direct measurement of quantum effi-ciency of single-photon emitters in hexagonal boron nitride," https://doi.org/10.1364/OPTICA.6.001084. It contains a distance-dependent lifetime measurement, a discussion on the used lifetime fit method, a single photon characterization, a discussion of the lifetime- and QE-fit stability, excitation wavelength dependent spectra, a far field polarization measurement and a corresponding simulation and further details on the sample preparation.**

## 1. LIFETIME AND QUANTUM EFFICIENCY MEASUREMENT

To determine the quantum efficiency, we related a change in local density of states (LDOS) to the changes in lifetime (see main text for detailed explanation). By approaching the single photon emitter (SPE) with a spherical mirror, a lifetime change could be observed. A typical lifetime - distance measurement can be seen in Figure S1 a). Corresponding lifetime measurements and fits at the marked extreme points are shown in b).

As described in the supplemental material of Ref. [1], we determined the excited state lifetime by recording time differences between the applied laser pulse and the photon arrival time at the avalanche photodiodes (APDs). A normalized histogram is shown in Figure S1 b). The fit represented by the solid line is given by a circular convolution (denoted by $*$) of a double exponential decay with the instrument response function (IRF):

$$f(\tau) = IRF * LT \tag{S1}$$

$$LT = a_1 e^{-t/\tau_1} + a_2 e^{-t/\tau_2} + b. \tag{S2}$$

With the amplitudes $a_1$ and $a_2$, the lifetimes $\tau_1$ and the fixed lifetime $\tau_2 = 0.5\,\text{ns}$ and the offset $b$.

Figure S1 c) and d) show the behavior of the described lifetime fit procedure with respect to an absolute number of counts used for the fit. These results indicate that the fit becomes reliable when more than 200 kcounts are taken into account. The data used for this estimate showed a short lifetime. Since short lifetimes are more difficult to determine, the results are considered upper limits. With this estimation we could calculate the necessary integration time for each emitter during the experiment simply by observing the count rate.

The resulting curves were fitted by Equation 1 and the substitution mentioned in Equation 2, giving

$$\tau(d) = \frac{\tau_\infty}{1 + \eta\left(\frac{P(\lambda, d+d_0)}{P(\lambda_0,\infty)} - 1\right)}, \tag{S3}$$

with the distance dependent lifetime $\tau$, the quantum efficiency $\eta$ and the wavelength and distance dependent dipole emission power $P(\lambda_0, \infty)$, extracted from simulations.

## 2. SINGLE EMITTER CHARACTERIZATION

Before a quantum efficiency measurement was performed, we verified that only one emitter was under observation. Besides observing only a single zero phonon line in the spectrum, a

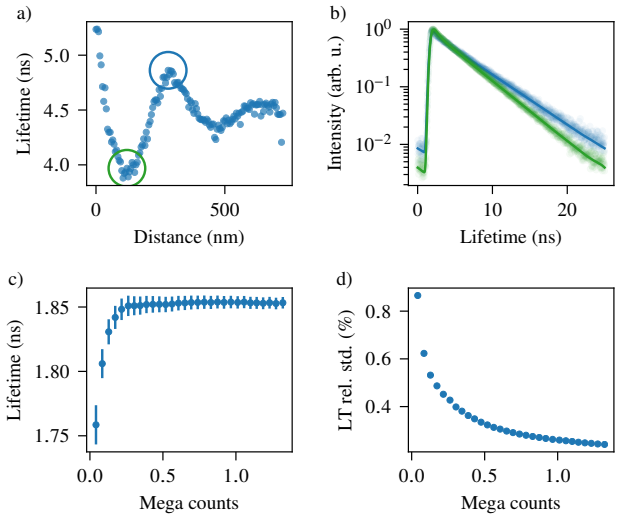


**Fig. S1.** *Quantum efficiency, corresponding lifetime measurement and reliability of the fit procedure.* a) Quantum efficiency measurement with 146 points and 6 s integration time per point, with an average count rate of 200 kcps. b) Lifetime measurement (dots) and fits (straight line), corresponding to a minimum (marked green in a) and b)) and a maximum (marked orange in a) and b)). c) Lifetime and d) corresponding relative standard deviation extracted from a fit with respect to number of detected photons. The fit converges when more than 200 kcounts are used.

normalized second order correlation function $g^{(2)}(\tau)$ was measured, as shown in Figure S2. The area below $g^{(2)}(\tau)$ over one repetition cycle $\tau_{\text{Rep.}}$ at a high delay time $\tau \to \infty$ gives an area of $\tau_{\text{Rep.}}$. To verify the single photon character of the collected light, the area under the zeroth peak has to be below $0.5\tau_{\text{Rep.}}$. In the example shown in Figure S2, this value is $(0.23 \pm 0.07)\ \tau_{\text{Rep.}}$.

## 3. EMITTER STABILITY

Since the QE measurements rely on the underlying lifetime measurements, we investigated temporal lifetime changes and the influence of an AFM tip approach. Figure S3 a) and b) show 400 s measurements in which we recorded photon arrival times of photons emitted by a single *h*-BN emitter. The time trace in a) shows the count rate binned to 10 ms sections. During this measurement the tip was retracted (separated by 7 µm) and occasionally approached, which can be seen by spikes in the count rate, as the tip acts as a mirror which increases the collection efficiency. The lifetime shown in b) was calculated from the same time stamps binned to 0.3 s sections. In contrast to the count rate, no correlation can be seen between the tip approaches and the determined lifetime. However, a slight gradual drift in lifetime over minutes could be observed.

This lifetime drift interferes with the QE measurement, adds noise and possibly changes the QE. Figure S3 c) shows a repeated measurement of the QE that scatters more than expected by the error bars. A lifetime drift on time scales longer than the measurement time of a single QE measurement could cause this effect. In contrast to the measurement series shown in the main text, no oscillations are recognizable, which is therefore assumed to be an artifact.

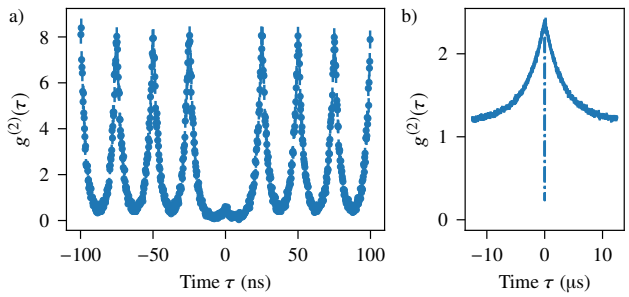


**Fig. S2.** *Second order coherence* The pulsed $g^{(2)}(\tau)$ function of the *h*-BN emitter (the emitter examined in Fig. 3 in the main text, at an excitation power of 56 µW) shows a clear antibunching, indicating for a single photon emission. a) and b) show the same pulsed $g^{(2)}(\tau)$ function with correlation times of 100 ns and 10 µs and resolutions of 0.25 ns and 25 ns. A bunching of several micro seconds can be seen.

## 4. ENERGY DEPENDENT SPECTRAL EMISSION

As already reported, another electronic level can be populated if the excitation energy is high enough [2]. This can have an influence on the lifetime (and thus QE) measurement, if this additional depopulation signal is fluorescent. The excitation wavelength dependent measurement shown in Fig. 3 a) (main text) remains unaffected by this, because no spectral changes could be observed by changing the excitation wavelength. A corresponding measurement is shown in Figure S4.

## 5. DIPOLE ORIENTATION

To reduce the free parameters needed to fit the quantum efficiency, i.e. Eq. 3 in the main text, we verified the horizontal alignment of the emitting dipole by a polarization measurement, analogous to what was described in the supplemental material of Ref. [1]. The fluorescence was guided through a $\lambda/2$ plate turned by the angle $\alpha/2$ and subsequently split by a polarizing beam splitter. Each output port was directed to an avalanche photo diode (APD). The recorded intensity will be denoted as $I_{\text{APD}_1}$ and $I_{\text{APD}_2}$. The relative intensity detected at one port is shown in Figure S5 a) and was calculated by (additionally we normalized the relative signal to its value averaged over $2\pi$, denoted by the horizontal line):

$$I_{\text{Norm}}(\alpha) = \frac{1}{2}\overline{\frac{I_{\text{APD}_1}}{I_{\text{APD}_1}+I_{\text{APD}_2}}}^{-1}\left(\frac{I_{\text{APD}_1}}{I_{\text{APD}_1}+I_{\text{APD}_2}}\right) \qquad \text{(S4)}$$

with the polarization angle $\alpha$. By fitting $I(\alpha) = I_{\text{min}} + (I_{\text{max}} - I_{\text{min}})\cos(\alpha - \phi)$ to the data (shown in Figure S5 a) as a solid line), the degree of polarization given by $\delta = (I_{\text{max}} - I_{\text{min}})/(I_{\text{max}} + I_{\text{min}}) = (0.797 \pm 0.001)$ arb. u. could be determined, analogous to Ref. [3]. Figure S5 b) shows the expected degree of polarization versus the out-of plane angle $\theta$, determined by a simulation of a dipole residing in the center of a 10 nm thick *h*-BN layer on top of a glass cover slide observed by a NA 1.4 objective lens. The maximal degree of polarization (only reached by a horizontally aligned dipole, i.e. $\theta = \pi/2$) is given by $\delta_{\text{Sim,Max}} = 0.82$, which is close to the measured value of $\delta = (0.797 \pm 0.001)$ arb. u.. Thus, we approximate the dipole to be horizontally aligned.

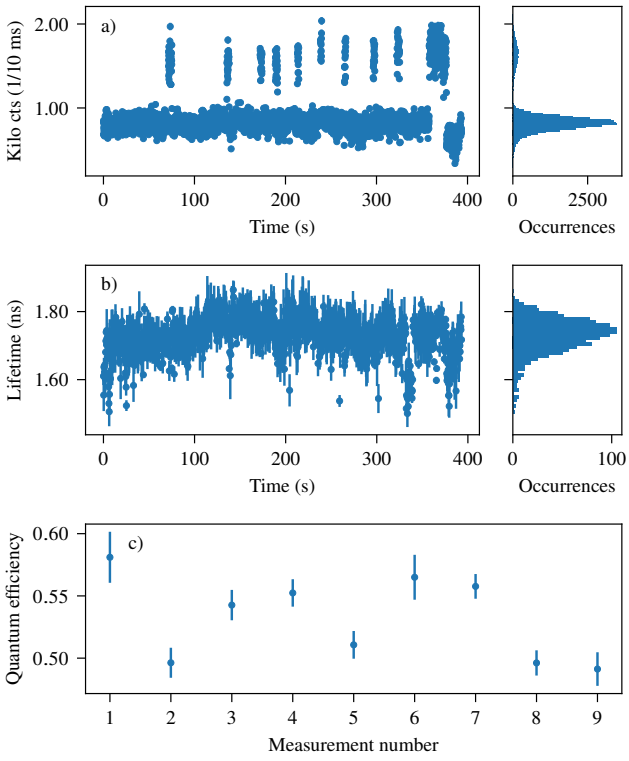


**Fig. S3.** *Lifetime drifts and a repeated quantum efficiency measurement.* Photon arrival times of a single *h*-BN emitter were recorded, while the gold covered sphere was occasionally approached. a) Time trace of the count rate, binned to 10 ms sections (every 10th bin is shown) and a corresponding histogram. A higher count rate indicate for a tip approach. b) Corresponding lifetime fits extracted from 0.3 s bins. c) A 10 times repetition of the quantum efficiency measurement on a *h*-BN emitter, analogous to Fig. 2 d). A smaller standard deviation of 0.03 was obtained by increasing the number of distance dependent lifetime measurement.

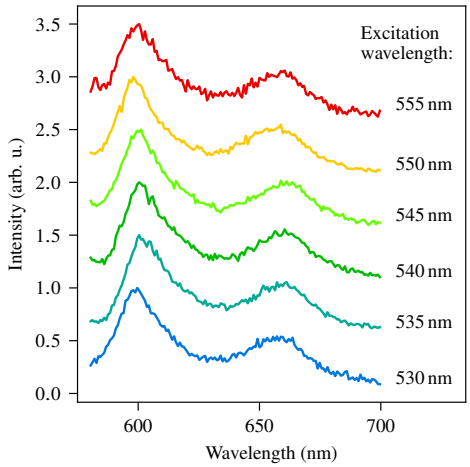


**Fig. S4.** *Excitation wavelength dependent emission spectra.* Spectra of the *h*-BN emitter studied in Fig. 3. a) (main text) recorded at different excitation wavelengths. No spectral changes could be found during the measurement.

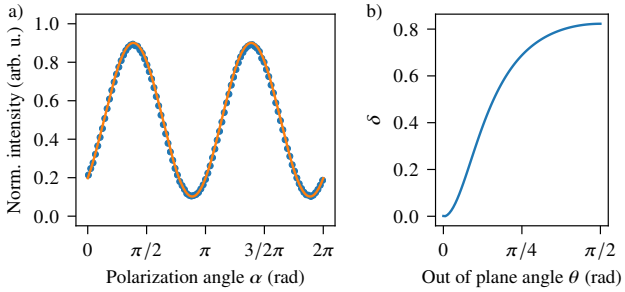


**Fig. S5.** *Polarization measurement and simulation.* a) Polarization measurement of a *h*-BN SPE, giving a degree of polarization of $\delta = (0.797 \pm 0.001)$ arb. u.. b) Simulation of the degree of polarization seen by a NA 1.4 oil immersion objective lens from a linear dipole in the middle of a 10 nm thick *h*-BN layer on top of a glass slide, giving a $\delta_{\text{Sim,Max}} = 0.82$ for a dipole parallel to the surface.

## 6. SAMPLE PREPARATION

*h*-BN was fabricated *via* a low pressure chemical vapor deposition process previously reported [4]. *h*-BN was grown on a copper catalyst, using ammonia borane as a precursor. The as-grown multi-layer *h*-BN films were then transferred to a glass coverslip *via* a PMMA assisted wet transfer process. The PMMA layer was then removed by soaking the sample in warm acetone overnight, before further cleaning by exposure to a UV-Ozone atmosphere for 20 min.

## REFERENCES

1. N. Nikolay, N. Mendelson, N. Sadzak, F. Böhm, T. T. Tran, B. Sontheimer, I. Aharonovich, and O. Benson, "Very Large and Reversible Stark Shift Tuning of Single Emitters in Layered Hexagonal Boron Nitride," ArXiv (2018).
2. A. W. Schell, M. Svedendahl, and R. Quidant, "Quantum Emitters in Hexagonal Boron Nitride Have Spectrally Tunable Quantum Efficiency," Adv. Mater. **30**, 1704237 (2018).
3. C. Lethiec, J. Laverdant, H. Vallon, C. Javaux, B. Dubertret, J.-M. Frigerio, C. Schwob, L. Coolen, and A. Maître, "Measurement of Three-Dimensional Dipole Orientation of a Single Fluorescent Nanoemitter by Emission Polarization Analysis," Phys. Rev. X **4**, 021037 (2014).
4. N. Mendelson, Z.-Q. Xu, T. T. Tran, M. Kianinia, J. Scott, C. Bradac, I. Aharonovich, and M. Toth, "Engineering and Tuning of Quantum Emitters in Few-Layer Hexagonal Boron Nitride," ACS Nano p. acsnano.8b08511 (2019).